Quantum Rod Emission Coupled to Plasmonic Lattice Resonances: A Collective Directional Source of Polarized Light

S. R. K. Rodriguez,[1, a)] G. Lozano,[1] M. A. Verschuuren,[2] R. Gomes,[3] K. Lambert,[3] B. De Geyter,[3, 4] A. Hassinen,[3] D. Van Thourhout,[4] Z. Hens,[3] and J. Gómez Rivas[1, 5]

[1)] *Center for Nanophotonics, FOM Institute AMOLF, c/o Philips Research Laboratories, High Tech Campus 4, 5656 AE Eindhoven, The Netherlands.*

[2)] *Philips Research Laboratories, High Tech Campus 4, 5656 AE Eindhoven, The Netherlands.*

[3)] *Physics and Chemistry of Nanostructures, Center for Nano and Biophotonics, Ghent University.*

[4)] *Photonics Research Group, Department of Information Technology, Ghent University-IMEC Sint-Pietersnieuwstraat 41, B-9000 Gent*

[5)] *COBRA Research Institute, Eindhoven University of Technology, P.O. Box 513, 5600 MB Eindhoven, The Netherlands*

(Dated: 13 January 2012)

We demonstrate that an array of optical antennas may render a thin layer of randomly oriented semiconductor nanocrystals into an enhanced and highly directional source of polarized light. The array sustains collective plasmonic lattice resonances which are in spectral overlap with the emission of the nanocrystals over narrow angular regions. Consequently, different photon energies of visible light are enhanced and beamed into definite directions.

[a)] Electronic mail: s.rodriguez@amolf.nl

The development of efficient and tunable (in photon energy, directionality, and polarization) nanoscale light emitters is a central goal for nanophotonics. Coupled semiconductor nanocrystal quantum emitters and metallic nanostructures offer an ideal platform for this purpose[1–3]: the emission energy can be tuned by varying the nanocrystal size due to quantum confinement of charge carriers, while the emitted light can be enhanced and controlled by structuring the metal to sustain surface plasmon polaritons which are resonant with the emission. It has been shown that Localized Surface Plasmon Resonances (LSPRs) in metallic nanoparticles may lead to a strong confinement of optical radiation into subwavelength volumes, resulting in a drastic modification of the emission spectra[4], and radiative decay rates[5], of emitters in this volume. However, such strong effects depend on an accurate positioning of the emitter in the region where the large electromagnetic enhancements occur. It is possible to overcome this position dependance by means of collective resonances in periodic arrays of metallic nanostructures. When a diffraction order is radiating in the plane of the array, i.e., at a Rayleigh anomaly condition, diffractive coupling of localized surface plasmons leads to collective, lattice-induced resonances known as Surface Lattice Resonances (SLRs)[6–10]. In contrast with LSPRs which typically manifest as broad spectral features in extinction with a flat angular dispersion, sharp and dispersive features in extinction may result from the excitation of SLRs[11]. The dispersive character of SLRs enables to design the interaction of the associated surface polaritons with light emitters in the vicinity of the array such that a resonant enhancement of the emission may take place over narrow spectral and angular regions. Moreover, the SLR polaritons extend over tens of microns[11], making it possible to obtain a collective enhancement of the emission from large volumes. In this Letter, we demonstrate that SLRs in an array of silver nanoantennas drastically modify the emission of a thin layer of randomly oriented CdSe/CdS core/shell Quantum Rods (QRs), rendering an enhanced and highly directional source of polarized light.

Silver nanoantenna arrays with a total size of 3×3 mm^2 were fabricated by Substrate Conformal Imprint Lithography (SCIL)[12] onto a fused silica substrate. A Scanning Electron Microscope (SEM) image of an array is shown in Figs. 1(a) and 1(b). This array has antennas with dimensions $340 \times 110 \times 20$ nm^3 arranged in a lattice with constants $a_x = 500$ nm and $a_y = 200$ nm. A 20 nm layer of Si_3N_4 was deposited on top of the array for a two-fold purpose: i) to passivate the silver, and ii) to serve as a spacer layer between the antennas and the QRs which prevents emission quenching[13,14]. The QRs were synthesized

following Carbone *et al.*[15]. They have diameters and lengths of 4.0 ± 0.6 and 36.1 ± 2.7 nm, respectively, and a Photoluminescence (PL) quantum yield of 65%. The absorbance and PL spectra of the QRs are shown in Fig. 1(c). We spin-coated a QR colloidal suspension of ca 11 microM on top of the Si_3N_4 layer, forming a compact layer of QRs [see inset of Fig. 1(c)] with a thickness of 60 nm.

We measured the variable angle zeroth-order extinction and PhotoLuminescence Enhancement (PLE) spectra of the structure. For the extinction measurements [see Fig. 1(a)], a p-polarized collimated beam from a halogen lamp impinged onto the sample, which we rotated around the x-axis while keeping the detector fixed. The transmission through the array, T_{in}, was normalized to the transmission outside the array (but through the substrate, Si_3N_4, and QRs layers), T_{out}, to obtain the zeroth order transmittance $T_0 = T_{in}/T_{out}$. The extinction, defined as $1 - T_0$, is shown in Fig. 2(a). The measurements in Fig. 2(a) are shown as a function of the photon energy and the in-plane component of the incident wave vector, $k_{\parallel} = k_0 \sin(\theta)\hat{y}$, where θ is the angle of incidence and $k_0 = \frac{2\pi}{\lambda_0}$ is the magnitude of the free space wave vector with λ_0 the vacuum wavelength. For the PLE measurements, [see Fig. 1(b)] the sample was excited by a continuous wave laser with an energy of 2.81 eV and an irradiance of 2 mW/mm^2 at a fixed angle of incidence $\theta = 5^{\circ}$. The pump irradiance was confirmed to be far below saturation by measurements not shown here. From the variable angle emission of the QRs inside the array I_{in}, and outside the array I_{out}, we obtained a PLE factor given by I_{in}/I_{out}. Figure 2(b) shows the PLE dispersion diagram for p-polarized emission in the main panel, and s-polarized emission in the inset. The measurements in Fig. 2(b) are shown as a function of the photon energy and the in-plane component of the wave vector of the emitted light. The white lines in Figs. 2(a) and 2(b) indicate the degenerate ($\pm$1,0) Rayleigh anomalies. They are calculated from the conservation of the parallel component of the wave vector, i.e., $k_{out}^2 = (k_x \pm m_1 G_x)^2 + (k_y \pm m_2 G_y)^2$, with k_{out} the magnitude of the scattered wave vector, $k_{\parallel} = (k_x, k_y)$ the wave vector components parallel to the surface, the integers (m_1, m_2) defining the order of diffraction, and $\vec{G} = (G_x = \frac{2\pi}{a_x}, G_y = \frac{2\pi}{a_y})$ the reciprocal lattice vector of the array. The array of antennas was assumed to be embedded in a homogeneous medium with n=1.45.

The broad peak in extinction near 2.07 eV in Fig. 2(a) corresponds to the LSPR for the short axis of the nanoantennas. Notice that its peak energy remains constant over the angular spectrum, which is a manifestation of the non-dispersive character of localized

resonances. The extinction also shows a pronounced dip near 1.69 eV at $k_{\|} = 0$, shifting towards higher energies for an inclined incidence. The good agreement between this dip and the calculated Rayleigh anomalies indicates that frequency dispersion of the surrounding medium is negligible, since a constant refractive index was assumed for the calculation. The coupling of the LSPR to the Rayleigh anomalies leads to narrow peaks in extinction on the low energy side of the Rayleigh anomalies, corresponding to the excitation of the $(\pm 1, 0)$ SLRs. As discussed in Ref.[16], the peak energy, dispersion, and linewidth of SLRs are determined by the coupling strength between the LSPR and the Rayleigh anomalies. The salient feature of the present system is that only until large values of $k_{||}$, the p-polarized SLRs cross in energy with the emission bandwidth of the QRs. For this reason, there is a resonant enhancement of the p-polarized emission by the SLRs at large values of $k_{||}$ only, as observed in the main panel in Fig. 2(b). Moreover, the PLE attains a dispersive character resembling the dispersion of the SLRs in extinction, i.e., the enhancement factor in the region where the quantum dots emit is roughly proportional to the extinction. The SLR enhanced emission is absent for s polarization [inset of Fig. 2(b)], where only a very weak feature (PLE ~ 1.3) near the Rayleigh anomaly condition is observed. The contrasting enhancement for s and p polarization arises from the plasmonic response of the nanoantennas, which determines the polarization dependent excitation of SLRs. We stress that although the Rayleigh anomalies have a purely geometrical origin and are therefore polarization independent, the excitation of the SLRs is determined by the shape and lattice dependent polarizability of the nanoantennas[6]. The different dimensions of the nanoantennas and the lattice along the x and y directions give rise to SLRs in the extinction spectra which overlap the emission of the QRs for p [see Fig. 2(a)], but not for s (not shown here) polarization. Therefore, the structure acts as an enhanced and directional source of p-polarized light.

In general, the total PLE may be factored into its contributions from the pump and emission energies[4,10]. We have verified that the influence of resonant pump enhancements is negligible by exciting the sample with different k-vectors and/or polarizations. Moreover, the total enhancement factor may slightly change for different pump conditions, but the features in the PLE dispersion diagram remain unchanged because the emission is molded by the dispersion of the SLRs at the emission energies. When considering the maximum 4-fold enhancement herein reported, it should be noted that we are starting with a fairly high quantum efficiency emitter. This condition makes large enhancement factors less feasible[17],

but demonstrates the possibility to improve and tailor the emission of an efficient light source.

In Figs. 3(a) and 3(b) we show cuts of the spectra in Figs. 2(a) and 2(b), with the blue solid, red dash-dotted, and green dashed lines corresponding to $k_{||} = 0$, $k_{||} = 7$ mrad/nm, and $k_{||} = 7.9$ mrad/nm, respectively. We observe that the emission is enhanced in the spectral regions close to where the extinction is highest, but the features appear to be shifted. We attribute this shift to the different excitation conditions in the extinction and PLE measurements. Namely, whereas the extinction corresponds to the removal of energy from an incident plane wave, the PLE corresponds to the out-coupled emission by the array when it is locally excited. Differences in the Far Field (FF) and Near Field (NF) spectra have been discussed in the context of emission [18] and extinction of electromagnetic radiation[19–21]. The extinction, which is determined by the FF interference, can be spectrally shifted with respect to the NF due to retardation effects. On the other hand, the loss of evanescent modes present in the NF interaction between the emitters and the antennas can change the FF emission spectra with respect to the NF spectra.

To further elucidate the modification of the emission spectra, we show in Fig. 3(c) the emission from the array, i.e. I_{in}, at the same values of $k_{||}$ of Figs. 3(a) and 3(b); the filled area is I_{out} at $k_{||} = 0$. For $k_{||} = 0$, where only the LSPR overlaps with the emission of the QRs, there is a blue shift of the peak emission energy. In contrast, a red shift occurs for large $k_{||}$, where the SLRs overlap with the emission of the QRs. In view of the size polydispersion of the QRs which determines the emission linewidth of the ensemble due to inhomogeneous broadening, we attribute the blue shifted emission to a stronger interaction of the smaller QRs with the LSPR, and the red shifted emission to a stronger interaction of the bigger QRs with the SLRs. To asses the angular modification of the emission by the array, we show in Figs. 3(d) and 3(e) I_{in} (dashed lines) and I_{out} (filled area) as a function of $k_{||}$ for two photon energies: (d) 1.89 eV and (e) 1.93 eV. Both I_{in} and I_{out} are normalized to the forward emission outside the array, i.e., the value of I_{out} at $\theta = 0$, for each energy. Outside the array the emission resembles a Lambertian emitter for both energies. Inside the array the emission is suppressed at low values of $k_{||}$, indicating that resonant pump enhancement is negligible, since the emission is quenched in the absence of a resonant emission enhancement. At large values of $k_{||}$, the emission is enhanced within a narrow angular bandwidth for a given energy, demonstrating the beaming of different emission energies into different directions.

In conclusion, we have shown how collective resonances in nanoantenna arrays enhance and modify light emission from semiconductor nanocrystals. By tailoring the spectral/angular overlap between surface lattice resonances and the emission spectra, we have demonstrated that a Lambertian emitter can be converted into a directional source of polarized light.

This work was supported by the Netherlands Foundation Fundamenteel Onderzoek der Materie (FOM) and the Nederlandse Organisatie voor Wetenschappelijk Onderzoek (NWO), and is part of an industrial partnership program between Philips and FOM. The work of S. R. K. R. was partially funded by an Erasmus Mundus Masters in Photonics scholarship.

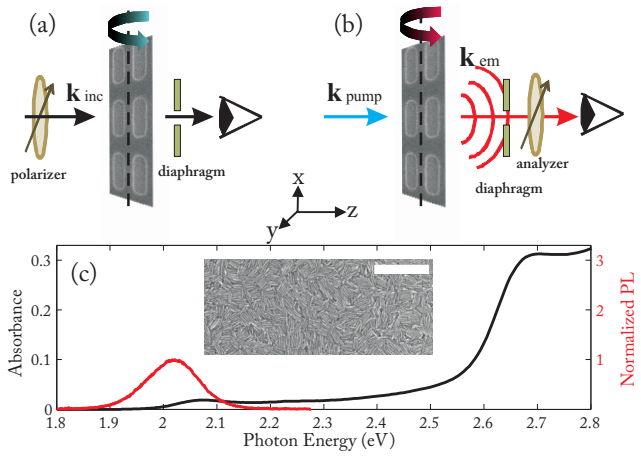

FIG. 1. Setup used for (a) Extinction, and (b) PL enhancement measurements. The sample is represented by a SEM image of a silver nanoantenna array, with the dashed lines indicating the axis of rotation for the sample in (a) and detector in (b). (c) Absorbance (left axis) and normalized PL (right axis) of CdSe/CdS core/shell quantum rods (QRs). The inset in (c) shows a SEM image of a spin-coated layer of QRs; the scale bar denotes 200 nm.

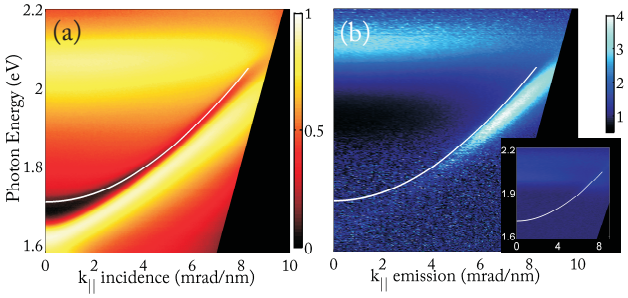

FIG. 2. (a) Extinction and (b - main panel) PL Enhancement angular spectra of p-polarized light of the sample described in the text. PL Enhancement of s-polarized light is shown in the inset of (b). The white lines indicate the degenerate (±1,0) Rayleigh anomalies.

REFERENCES

[1]J. N. Farahani, D. W. Pohl, H.-J. Eisler, and B. Hecht, Phys. Rev. Lett. **95**, 017402 (2005).

[2]A. G. Curto, G. Volpe, T. H. Taminiau, M. P. Kreuzer, R. Quidant, and N. F. van Hulst, Science **329** (2010).

[3]H. Mertens, J. S. Biteen, H. A. Atwater, and A. Polman, Nano Lett. **6**, 2622 (2006).

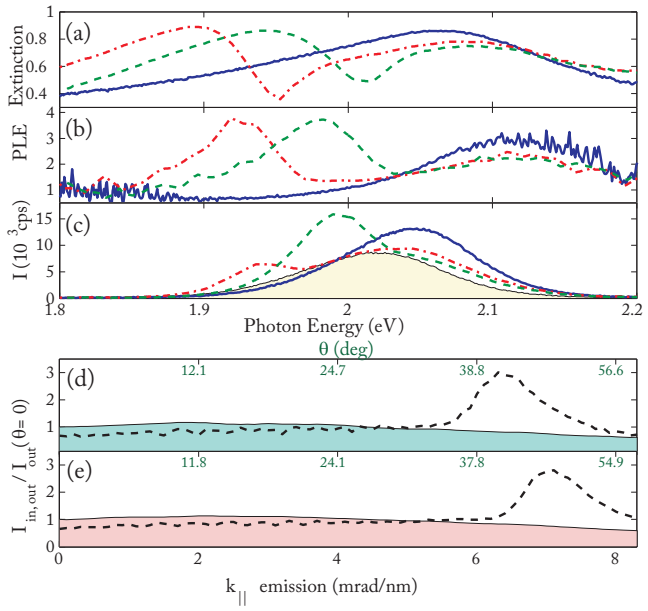

FIG. 3. (a) Extinction, (b) PL Enhancement, and (c) emission inside the array, i.e. I_{in}, in 10^3 counts per second, at $k_{||} = 0$ (blue solid lines), $k_{||} = 7$ mrad/nm (red dash-dot lines), and $k_{||} = 7.9$ mrad/nm (green dashed lines). The filled area in (c) is the emission outside the array, i.e. I_{out}, at $k_{||} = 0$; I_{out} for the larger values of $k_{||}$ (not shown here) has the same line shape as in $k_{||} = 0$, but with a lower amplitude. (d) and (e) show the angular dependent emission for an energy of (d) 1.89 eV, and (e) 1.93 eV, with I_{in} as black dashed lines and I_{out} as a filled area. Both I_{in} and I_{out} are normalized to the value of I_{out} at $\theta = 0$ for each energy. The upper ticks indicate the value of the emission angle θ corresponding to the $k_{||}$ values in the x-axis. All measurements are shown for p-polarized light.

[4]M. Ringler, A. Schwemer, M. Wunderlich, A. Nichtl, K. Kürzinger, T. A. Klar, and J. Feldmann, Phys. Rev. Lett. **100**, 203002 (2008).

[5]O. L. Muskens, V. Giannini, J. A. Sánchez-Gil, and J. Gómez Rivas, Nano Lett. **7**, 2871 (2007).

[6]S. Zou, N. Janel, and G. C. Schatz, J. Chem. Phys. **120**, 10871 (2004).

[7]Y. Chu, E. Schonbrun, T. Yang, and K. B. Crozier, Appl. Phys. Lett. **93**, 181108 (2008).

[8]B. Auguié and W. L. Barnes, Phys. Rev. Lett. **101**, 143902 (2008).

[9]V. G. Kravets, F. Schedin, and A. N. Grigorenko, Phys. Rev. Lett. **101**, 087403 (2008).

[10]G. Vecchi, V. Giannini, and J. Gómez Rivas, Phys. Rev. Lett. **102**, 146807 (2009).

[11]G. Vecchi, V. Giannini, and J. Gómez Rivas, Phys. Rev. B **80**, 201401 (2009).

[12]M. A. Verschuuren, Substrate Conformal Imprint Lithography for Nanophotonics, PhD dissertation, Utrecht University (2010).

[13]A. Wokaun, H.-P. Lutz, A. P. King, U. P. Wild, and R. R. Ernst, J. Chem. Phys. **79**, 509 (1983).

[14]P. Anger, P. Bharadwaj, and L. Novotny, Phys. Rev. Lett. **96**, 113002 (2006).

[15]L. Carbone, C. Nobile, M. De Giorgi, F. D. Sala, G. Morello, P. Pompa, M. Hytch, E. Snoeck, A. Fiore, I. R. Franchini, M. Nadasan, A. F. Silvestre, L. Chiodo, S. Kudera, R. Cingolani, R. Krahne, and L. Manna, Nano Lett. **7**, 2942 (2007).

[16]S. R. K. Rodriguez, A. Abass, B. Maes, O. T. A. Janssen, G. Vecchi, and J. Gómez Rivas, Phys. Rev. X **1** (2011).

[17]D. A. Weitz, S. Garoff, J. Gersten, and A. Nitzan, J. Chem. Phys. **78**, 5234 (1983).

[18]A. V. Shchegrov, K. Joulain, R. Carminati, and J.-J. Greffet, Phys. Rev. Lett. **85** (2000).

[19]G. Bryant, F. J. Garcia de Abajo, and J. Aizpurua, Nano Lett. **8**, 631 (2007).

[20]B. M. Ross and L. P. Lee, Opt. Lett. **34**, 896 (2009).

[21]V. Giannini, G. Vecchi, and J. Gómez Rivas, Phys. Rev. Lett. **105**, 266801 (2010).